

Perturbative QCD coherence in e^+e^- annihilation

G. Kramer¹ and G.A. Schuler²

¹ II. Institut für Theoretische Physik*, Universität, D-2000 Hamburg, Federal Republic of Germany

² Deutsches Elektronen-Synchrotron (DESY), D-2000 Hamburg, Federal Republic of Germany

Received 11 May 1988

Abstract. We study the pattern of soft parton radiation in the hard annihilation processes $e^+e^- \rightarrow q\bar{q}\gamma$ and $e^+e^- \rightarrow q\bar{q}g$ by explicit evaluation of the cross sections for $e^+e^- \rightarrow q\bar{q}\gamma g$ and $e^+e^- \rightarrow q\bar{q}gg + q\bar{q}q\bar{q}$ taken care of correct normalization. We find the coherence effects as observed experimentally and discuss why these effects are not present in the usual models based on $O(\alpha_s^2)$ perturbation theory with subsequent independent fragmentation.

1 Introduction

It is generally agreed upon that experimental data in high energy e^+e^- annihilation into hadrons are very well described by the production of up to four partons, either quarks, antiquarks or gluons as predicted by QCD perturbation theory with subsequent fragmentation of the produced partons into final state hadrons [1]. This fragmentation or hadronization can be described only by phenomenological models, in which the hadrons are created with limited transverse momenta. This automatically leads to jet production at high energies. The first fragmentation model used in this connection was the so-called independent fragmentation model (IF). In this model the original description of Field and Feynman [2] for single quark fragmentation is extended to each parton individually. The gluon is treated either as a quark [3] or split into a quark-antiquark pair [4]. With both of these two models the bulk of the experimental data can be accounted for. But there is at least one observation which cannot be described in independent fragmentation models, the so-called string effect, first detected by the JADE collaboration [5] and later confirmed by several other experiments [6]. The string effect is as follows:

Selecting the hardest jet in 3-jet events the particle density with respect to the direction of this jet is higher in the region between the most energetic jet and the least energetic jet as compared to the particle density in the region between the two most energetic jets. The least energetic jet is most probably the gluon jet in the 3-jet sample. With other words the particle density between quark and antiquark jet is depleted as compared to the regions between gluon and quark or antiquark jet, respectively. The gross features of the particle (or energy) flow between the jets come out correctly also in IF models. Nevertheless it is usually concluded that due to the insufficient depletion of particles between the two most energetic jets IF models should be discarded. The Lund or string fragmentation (SF) model [7], on the other hand, describes the observed string effect very well. Actually it was predicted in this model before it was experimentally found. In this model the gluon is part of a string stretched between quark and antiquark. If the gluon is soft its main effect is to give some small transverse momentum to the string and the events remain 2-jet like. If the gluon has large energy and is emitted at a large angle with respect to the quark and antiquark it will give a large transverse momentum to the string and generate 3-jets. However, since the gluon is connected via the string to the quark and antiquark it will drag both string pieces in the direction of the gluon and thus depleting the particle density in the opposite region between quark and antiquark.

Some time ago Azimov et al. advanced a novel explanation of the string effect already on the parton level [8]. Although the phenomenon of the string effect occurs experimentally in the angular flow of hadrons between jets they argued that there is a close correspondence between the angular distribution of soft parton and hadron flows, and therefore the string effect should be visible already in the angular distribution of soft partons emitted from three hard parton jets. They demonstrated this effect by calculating the coherent gluon radiation of colour antenna consisting

* Supported by Bundesministerium für Forschung und Technologie, 05 4HH 92P/3, Bonn, FRG

of three emitters, namely quark, antiquark and gluon whose directions were fixed as in the experimental situation. In addition they showed that for $e^+e^- \rightarrow q\bar{q}\gamma$ the emission of an additional gluon projected into the $q\bar{q}\gamma$ plane does not produce the interference effect in the region between q and \bar{q} jet. The distribution on the side where the hard photon is emitted is approximately equal to the distribution on the opposite side. These predictions have been confirmed by the TPC [9], MARK II [10] and JADE [11] collaborations. By considering the ratio of the angular dependence of hadrons emitted between q and \bar{q} for $q\bar{q}g$ and $q\bar{q}\gamma$ events the coherence effect could be demonstrated without relying on model calculations. This ratio would be one if no coherence effects were present, since the gluon and photon energies were chosen such that the kinematic configuration of both event types were approximately equal. In the $q\bar{q}g$ events the $q\bar{q}$ region is defined as the region between the two most energetic jets.

The string effect occurs also in parton shower fragmentation models [12]. In these models the depletion of particle emission in the $q\bar{q}$ region originates from the angular ordering of soft gluon emission in the parton cascades. This angular ordering introduces interference effects in an originally incoherent emission process [13].

It is well known that the cross section for gluon emission in the limit of one of the gluons being soft ($k \rightarrow 0$) factorizes into the cross section for the hard process (i.e. the process without the extra soft gluon) and an eikonal factor for each hard parton from which a soft gluon can be emitted [14]. If three partons $q\bar{q}g$ ($q\bar{q}\gamma$) are held fixed into a 3-jet (2-jet) configuration and if the second (first) gluon becomes soft then the cross section for $e^+e^- \rightarrow q\bar{q}gg$ ($q\bar{q}\gamma g$) results in the formulas of Azimov et al. [8], from which the coherence of gluon emission was deduced.

In all models based on $O(\alpha_s^2)$ QCD perturbation theory [15] the contributions of $e^-e^- \rightarrow q\bar{q}gg + q\bar{q}q\bar{q}$ are fully taken into account. Then we might expect that the coherence effect in the form proposed by Azimov et al. [8] should be present and the string effect built in to the Lund fragmentation would be unnecessary.

In this paper we want to study under which circumstances the coherence pattern already present in second order QCD perturbation theory can be built into models based on QCD matrix elements. For this purpose, we collect the formulas for $e^+e^- \rightarrow q\bar{q}gg$ taking only the most singular terms and compare them with the results in [8]. This is done in Sect. 2. With these formulas we calculate the angular distribution of an additional soft gluon emitted in $e^+e^- \rightarrow q\bar{q}\gamma$ and $e^+e^- \rightarrow q\bar{q}g$ with fixed 2- ($q\bar{q}$) or 3-jet ($q\bar{q}g$) kinematics as a function of the energy and the polar angle of the soft gluon. These results are compared to those obtained with the complete cross section $e^+e^- \rightarrow q\bar{q}gg + q\bar{q}q\bar{q}$, i.e. without the approximation of

taking only the most singular terms. We study for comparison also the case of an abelian gluon theory. The actual realizations of $O(\alpha_s^2)$ models require the introduction of resolution cuts [15]. Therefore it is important to investigate how the soft gluon distribution behaves as a function of these cut values. Section 3 contains a summary and some concluding remarks.

2 Soft gluon emission cross section

The distribution of one single soft gluon with momentum p_3 is calculated from the $O(\alpha_s^2)$ four-parton cross section for $e^+e^- \rightarrow q(p_1) + \bar{q}(p_2) + g(p_3) + g(p_4)$ which we write in the form

$$d\sigma = \sigma_0 \frac{2\pi}{q^2} \int \prod_{i=1}^4 \frac{d^3 p_i}{(2\pi)^3 2E_i} \cdot (2\pi)^4 \delta^{(4)}\left(q - \sum_{i=1}^4 p_i\right) (-g^{\mu\nu} \tilde{H}_{\mu\nu}) \quad (2.1)$$

where the hadron tensor $H_{\mu\nu}$ has been written as

$$H_{\mu\nu} = N_c \sum_{i=1}^{N_f} e_i^2 \tilde{H}_{\mu\nu} \quad (2.2)$$

so that the quark charges e_i and the factor N_c are absorbed in the lowest order cross section σ_0 . Following [16] the phase space is expressed by the scaled energies $x_i = 2E_i/\sqrt{q^2}$ ($i = 1, 2, 3, 4$), the angle θ_{34} , i.e. the angle between the two gluon momenta \vec{p}_3 and \vec{p}_4 , and the azimuth angle ϕ which is the angle of \vec{p}_3 projected into the plane perpendicular to $\vec{p}_3 + \vec{p}_4$:

$$d\sigma = \sigma_0 \frac{q^2}{128(2\pi)^5} \frac{x_4(x_4 + x_3)(x_4 + x_3 \cos \theta_{34})}{(x_4^2 + 2x_3x_4 \cos \theta_{34} + x_3^2)^{3/2}} \cdot dx_1 dx_2 x_3 dx_3 d \cos \theta_{34} d\phi (-g^{\mu\nu} \tilde{H}_{\mu\nu}). \quad (2.3)$$

The first part of the phase space in (2.3) is exactly the three-jet phase space with jet energies x_1, x_2 and $2 - x_1 - x_2 \simeq x_4$ (for x_3 small) while the remainder represents the relative parton distribution inside a three-jet event.

As in [8] we define new angles θ_3 and ϕ_3 . θ_3 is the polar angle of \vec{p}_3 with respect to the axis in the direction $\vec{p}_1 \times \vec{p}_2$ and ϕ_3 is the azimuthal angle of \vec{p}_3 in the \vec{p}_1, \vec{p}_2 -plane with $\phi_3 = 0$ when \vec{p}_3 is in the direction of \vec{p}_1 . We have

$$d \cos \theta_{34} d\phi = d \cos \theta_3 d\phi_3 \quad (2.4)$$

so that the correctly normalized soft-gluon distribution is calculated from

$$d\sigma = \sigma_0 \frac{q^2}{128(2\pi)^5} \frac{x_4(x_4 + x_3)(x_4 + x_3 \cos \theta_{34})}{(x_4^2 + 2x_3x_4 \cos \theta_{34} + x_3^2)^{3/2}} \cdot dx_1 dx_2 x_3 dx_3 d \cos \theta_3 d\phi_3 (-g^{\mu\nu} \tilde{H}_{\mu\nu}). \quad (2.5)$$

The transition matrix elements for the processes $e^+e^- \rightarrow q\bar{q}gg$ and $e^+e^- \rightarrow q\bar{q}q\bar{q}$ have been given in [17, 18]. We decompose them into the colour factors

C_F^2 , $C_F N_c$ and $C_F T_R$. First we consider the most singular contributions to (2.5), which are calculated in the limit that gluon 3 is soft and/or collinear with the quark or antiquark ($y_{13} \rightarrow 0$):

$$d\sigma = \sigma_0 \left(\frac{\alpha_s}{2\pi} \right)^2 B(x_1, x_2) \left\{ \frac{2C_F(C_F - N_c/2)y_{12}}{y_{13}y_{23}} + C_F^2 \left[\frac{1}{y_{13}y_{12} + y_{23}} + \frac{1}{y_{23}y_{12} + y_{13}} \right] \right\} \cdot \frac{x_3}{4} dx_3 \frac{d\phi_3}{2\pi} d\cos\theta_3 dx_1 dx_2. \quad (2.6)$$

The extra kinematical factor in (2.5) which depends on x_4, x_3 and $\cos\theta_{34}$ has been replaced by 1, i.e. its limit for $x_3 \rightarrow 0$. In (2.6)

$$B(x_1, x_2) = \frac{x_1^2 + x_2^2}{(1-x_1)(1-x_2)} \quad (2.7)$$

is the Born term for $e^+e^- \rightarrow q\bar{q}g$. In terms of four-parton variables we have $x_1 = 1 - y_{24}$, $x_2 = 1 - y_{134}$, $x_4 = 2 - x_1 - x_2 = 1 - y_{123}$ with $y_{ij}q^2 = (p_i + p_j)^2$ and $y_{ijk}q^2 = (p_i + p_j + p_k)^2$ as usual. These relations between four-parton momenta and three-jet momenta are correct only in the limit $y_{13} \rightarrow 0$.

For $N_c = 0$ and $(C_F\alpha_s)^2 \rightarrow e_f^2 C_F\alpha_s\alpha$ in (2.6) this formula gives us the cross section for $e^+e^- \rightarrow q\bar{q}g\gamma$, where the soft gluon has momentum p_3 and the hard photon, which produces the ‘‘third jet,’’ has momentum p_4 . The coupling depends on the quark charge e_f . Formula (2.6) agrees up to normalization with the corresponding formula for $e^+e^- \rightarrow q\bar{q}g\gamma$ in Azimov et al. [8] if we neglect the single pole terms in (2.6). This corresponds to the most singular term in the limit y_{13} and $y_{23} \rightarrow 0$, which is the soft gluon limit $x_3 \rightarrow 0$. Then the cross section factorizes into the cross section for $e^+e^- \rightarrow q\bar{q}\gamma$ and the eikonal factor which is equal to $2y_{12}/y_{13}y_{23}$. Our cross section has the correct normalization with the replacement of couplings above. Of course, if several flavours are produced we must take the sum over flavours f . Equation (2.6) gives the four-parton cross section in the limit $y_{13} \rightarrow 0$ only. If the momentum x_3 of the soft gluon is chosen very small we expect (2.6) to be a very good approximation to the complete cross section. We have calculated the distributions also for the complete cross section formula in order to test the singular approximation (2.6). However, outside the limiting region $y_{13} \rightarrow 0$ the relations between 4-parton variables and the 3-jet variables x_1, x_2 and x_4 are ambiguous [18]. The relation between the 4-parton energies $x_i (i=1, \dots, 4)$ and the invariants y_{ijk} is as follows $x_1 = 1 - y_{234}$, $x_2 = 1 - y_{134}$, $x_3 = 1 - y_{124}$, $x_4 = 1 - y_{123}$. For $x_3 = 0$ we have as three-jet energies $x_1 = 1 - y_{24}$, $x_2 = 1 - y_{14}$, $x_4 = 1 - y_{12}$ with $x_3 = 1 - y_{12} - y_{14} - y_{24} = 2 - x_1 - x_2 - x_4 = 0$ following from energy conservation for three jets. Since $x_3 \neq 0$ we make a choice for the 3-jet energies x_I, x_{II}, x_{III} as follows:

$$x_I = x_1 + x_3$$

$$x_{II} = x_2$$

$$x_{III} = x_4. \quad (2.8)$$

Before we proceed to the additional $C_F N_c$ contributions we evaluate (2.6) and the corresponding complete C_F^2 expression as a function of ϕ_3 for fixed x_I, x_{II} and $x_{III} = 2 - x_I - x_{II}$, following the experimental selection of the jet events. x_3 is chosen small compared to x_I, x_{II} and x_{III} and θ_3 is integrated over $0 \leq \theta_3 \leq \pi$. In (2.8) it is arbitrary in which form x_3 is attributed to x_1, x_2 or x_4 . For $\theta_3 = \pi/2$ all four partons including the soft gluon are emitted in a plane. The invariants y_{ij} written in terms of x_i, x_j and the angle θ_{ij} are:

$$y_{ij} = \frac{x_i x_j}{2} (1 - \cos\theta_{ij}) \quad (2.9)$$

where $i, j = 1, 2; 1, 3; 1, 4; 2, 3; 2, 4$ and $3, 4$. The angles θ_{12}, θ_{14} and θ_{24} are fixed by the three-jet kinematics, i.e.

$$\cos\theta_{12} = 1 - \frac{2}{x_I x_{II}} (x_I + x_{II} - 1) \quad (2.10)$$

and similarly for θ_{14} and θ_{24} . The angles θ_{13}, θ_{23} and θ_{34} vary with ϕ_3 according to [8]:

$$\begin{aligned} \cos\theta_{13} &= \cos\phi_3 \sin\theta_3 \\ \cos\theta_{23} &= \cos(\theta_{12} - \phi_3) \sin\theta_3 \\ \cos\theta_{34} &= \cos(\theta_{14} - \phi_3) \sin\theta_3. \end{aligned} \quad (2.11)$$

It is clear that all these relations are correct only for $x_3 \rightarrow 0$. For exact 4-parton kinematics, $x_3 \neq 0$, θ_{24} and θ_{34} are related to the other angles by

$$\begin{aligned} \cos\theta_{34} &= (x_1^2 + x_2^2 + 2x_1 x_2 \cos\theta_{12} - x_4^2 - x_3^2)/2x_3 x_4 \\ \cos\theta_{24} &= (x_1^2 + x_3^2 + 2x_1 x_3 \cos\theta_{13} - x_2^2 - x_4^2)/2x_2 x_4 \end{aligned} \quad (2.12)$$

which is compatible with (2.10) and (2.11) if $x_3 \rightarrow 0$.

The results for $e^+e^- \rightarrow q\bar{q}g\gamma$ follow directly from (2.6) with (2.8), (2.10) and (2.11). We plot them as calculated from (2.6) with $N_c = 0$, $C_F = 1$ without the additional factor $e_f^2 \alpha$ for easier comparison with results for $e^+e^- \rightarrow q\bar{q}gg$. So, to obtain correctly normalized $q\bar{q}\gamma(g)$ cross sections we must multiply our curves with $\alpha \Sigma_f e_f^4 / \alpha_s \Sigma_f e_f^2 = 35\alpha/99\alpha_s$ if we include up to five flavours. We have chosen $\alpha_s = 0.15$ and the normalized jet energies similar to the jet energies in the experiments [9, 10, 11]: $x_I = 0.876$, $x_{II} = 0.703$, $x_{III} = 0.421$. The corresponding jet angles are $\theta_{12} = 151.70^\circ$, $\theta_{14} = 232.42^\circ$ and $\theta_{24} = 80.72^\circ$. For x_3 we take the values $x_3 = 0.05, 0.1$ and 0.2 . The last value is presumably outside the range where (2.6) is a good approximation. We have selected it in order to see the deviations of (2.6) from exact 4-parton matrix elements. Remember that (2.6) is correct only in the limit $y_{13} \rightarrow 0$. For y_{13} large many more term are present.

In Fig. 1 we show the comparison between the approximate cross section as given by (2.6) without the single pole terms in y_{13} and y_{23} and the exact

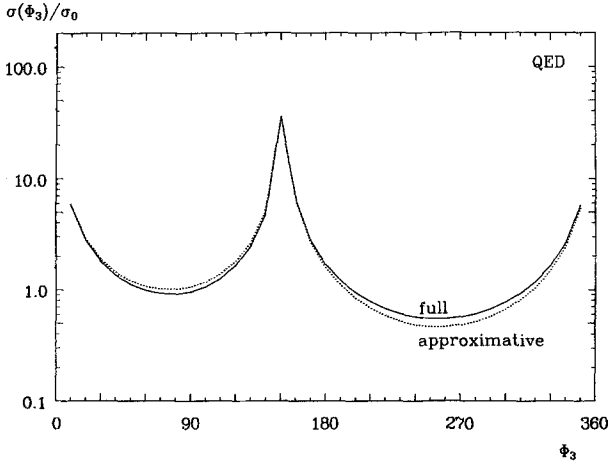


Fig. 1. The soft gluon angular distribution $\sigma(\phi_3)/\sigma_0$ between q and \bar{q} in $q\bar{q}\gamma$ events (integrated over θ_3 and for $x_3 = 0.2$) for complete matrix elements (full) and for the most singular approximation (approximative) as a function of ϕ_3

expression where all C_F^2 terms are included. But we left out the kinematic factor in (2.5) which goes to 1 for $x_3 \rightarrow 0$. To neglect the nonleading terms in x_3 in the kinematical factor but to retain them in the cross section matrix elements is somewhat inconsequent. If we want to retain the full kinematic factor we cannot factorize the cross section into the cross section for $e^+e^- \rightarrow q\bar{q}\gamma$ and a kinematical factor as we have done it. Then the complete cross section for $e^+e^- \rightarrow q\bar{q}\gamma g$ would make a more complicated analysis necessary. We also emphasize that the reduction of 4-parton kinematics to 3-jet kinematics and an independent second gluon is only valid in the limit $x_3 \rightarrow 0$. In Fig. 1 and in all following figures we plot $\sigma(\phi_3)/\sigma_0 = (d^4\sigma/dx_1 dx_2 dx_3 d\phi_3/2\pi)/\sigma_0$. The photon is emitted in the interval of ϕ_3 between $\phi_3 = \theta_{12}$ and $\phi_3 = 2\pi$. We have integrated over θ_3 in $0 \leq \theta_3 \leq \pi$.

As expected the cross section has two maxima at $\phi_3 = 0$ and $\phi_3 = \theta_{12}$ where y_{13} and y_{23} vanish. Through interference of the y_{13} pole with the y_{23} pole in (2.6) the minimum between $\phi_3 = \theta_{12}$ and $\phi_3 = 2\pi$ is deeper than the minimum between $\phi_3 = 0$ and $\phi_3 = \theta_{12}$. This qualitative feature is also seen in the experimental data. In Fig. 1 we took $x_3 = 0.2$. We see that the approximate formula (2.6) is quite good even for $x_3 = 0.2$. The deviation is of order of 20% at the minima. Thus the ratio r of the minimum between $\phi_3 = 0$ and $\phi_3 = \theta_{12}$ to the minimum between $\phi_3 = \theta_{12}$ and $\phi_3 = 2\pi$ changes only from $r \simeq 2.3$ to $r \simeq 1.7$ if the exact matrix elements are used.

The dependence of the ϕ_3 distribution on x_3 is shown in Fig. 2 where we have plotted results for $x_3 = 0.05, 0.1$ and 0.2 . It is clear that the cross section increases if x_3 is lowered. The ratio $r = \sigma(\phi_3/\phi_{12})/\sigma(\phi_3/\phi_{21})$ as a function of ϕ_3/ϕ_{12} , where $\phi_{12} = \theta_{12}$ and $\phi_{21} = 2\pi - \phi_{12}$ is shown in Fig. 3. We see that r in the minima changes from $r = 1.68$ at $x_3 = 0.2$ to $r = 1.98$ at $x_3 = 0.05$. $r > 1$ occurs also in the experimental soft

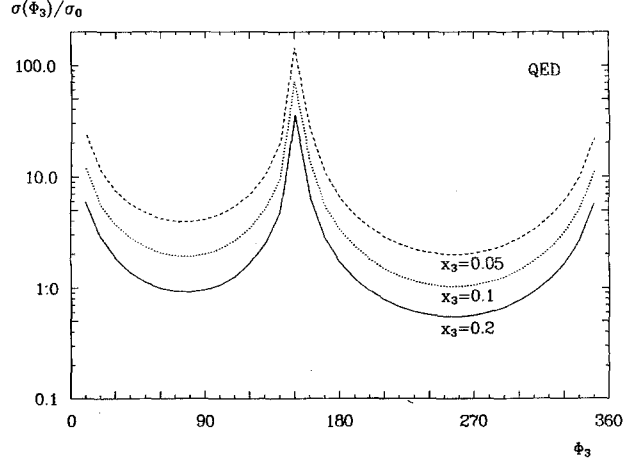


Fig. 2. $\sigma(\phi_3)/\sigma_0$ between q and \bar{q} for $q\bar{q}\gamma$ events for $x_3 = 0.05, 0.1$ and 0.2 (complete matrix elements) as a function of ϕ_3

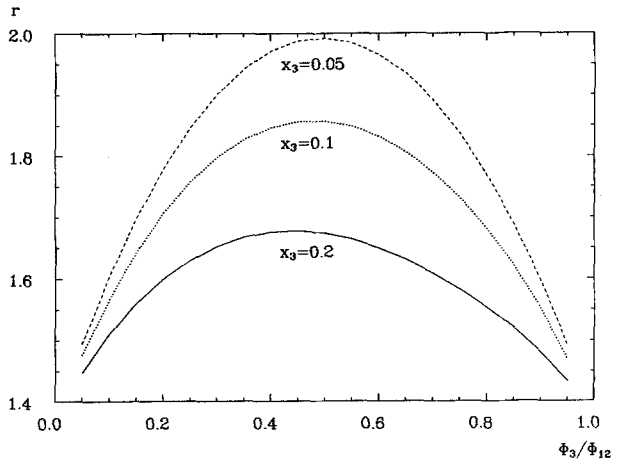


Fig. 3. The ratio r of soft gluon densities in $q\bar{q}\gamma$ events as a function of the normalized angle ϕ_3/ϕ_{12} for $x_3 = 0.05, 0.1$ and 0.2

particle distributions for 2-jet-one photon events: $r \simeq 2$ to 3 for the TPC [19], MARK II [10] and JADE [11] distributions.

Now we come to the remaining $C_F N_c$ contributions which together with the terms already contained in (2.6) give all the $C_F N_c$ terms. Actually the contribution of (2.6) to the full QCD cross section is not very important since $C_F \simeq N_c/2$, so that the contribution of (2.6) is diminished. The dominant $C_F N_c$ terms in the singular approximation $y_{34} \rightarrow 0$ is

$$d\sigma = \sigma_0 \left(\frac{\alpha_s}{2\pi} \right)^2 B(x_1, x_2) C_F N_c \cdot \left\{ \frac{y_{14}}{y_{13} y_{34}} + \frac{y_{24}}{y_{23} y_{34}} + \frac{1}{2} \frac{y_{23}}{y_{34} y_{23} + y_{24} y_{23} + y_{24}} \right\} \cdot \frac{x_3}{4} dx_3 \frac{d\phi_3}{2\pi} d \cos \theta_3 dx_1 dx_2, \quad (2.14)$$

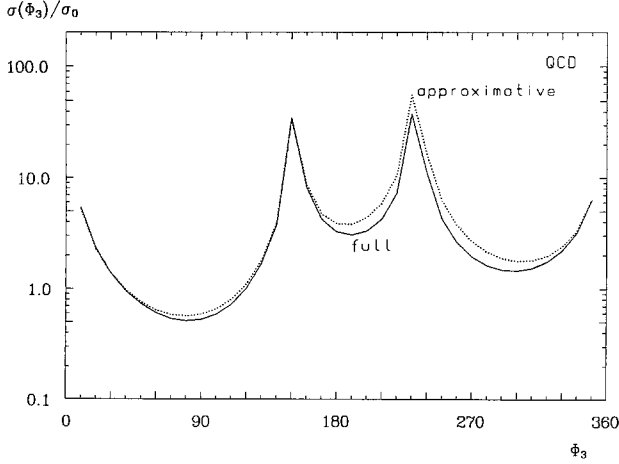


Fig. 4. The soft parton angular distribution $\sigma(\phi_3)/\sigma_0$ between q , \bar{q} and g in $q\bar{q}g$ events (integrated over θ_3 and for $x_3 = 0.2$) for complete matrix elements (full) and for the most singular approximation (approximative) as a function of ϕ_3

The three-jet energies are now $x_I = x_1 = 1 - y_{234}$ and $x_{II} = x_2 = 1 - y_{134}$ and $x_{III} = x_3 + x_4$. In (2.14) the first and second term with double poles in y_{34} and y_{13} and in y_{34} and y_{23} , respectively, are the important terms. They produce the characteristic interference pattern for the soft gluon emission between the three jets. They correspond to the eikonal approximation and are obtained in the soft limit $x_3 \rightarrow 0$. First we have studied the difference between the approximate formula (2.14) (without the single y_{34} pole terms) which agrees with the formulas in [8], up to normalization, and the complete matrix element with all non-singular contributions included. This is shown in Fig. 4 with $x_3 = 0.2$. In Fig. 4 we see the three-jet structure. The first maximum at $\phi_3 = \theta_{12}$ is the \bar{q} -jet (q is at $\phi_3 = 0, 2\pi$) and the maximum at $\phi_3 = \theta_{14}$ is the hard gluon jet. The first minimum, between q and \bar{q} jet is deepened through the interference in the double pole $1/y_{13}y_{34}$ in (2.14), whereas the second minimum between \bar{q} and g jet is pushed upwards caused by the constructive interference in $1/y_{23}y_{34}$. The third minimum is also pushed upwards as compared to the $q\bar{q}\gamma$ case through constructive interference coming from the $1/y_{13}y_{34}$ double pole. The difference between the exact formula and the most singular approximation is largest at the minima, of the order of 30%. The curve for the singular approximation lies always above the exact curve (this was not the case for $q\bar{q}\gamma$, see Fig. 1). The x_3 dependence of the ϕ_3 distribution is shown in Fig. 5. For decreasing x_3 the cross section increases like $1/x_3$. The curves are for $x_3 = 0.05, 0.1$ and 0.2 . The cross section in the minima are approximately in the relation 1:7:3, roughly independent of x_3 . In the experimental data for the soft hadron distribution this relation is approximately 1:6:2 [11] which agrees quite nicely with the theoretical ratio.

Comparing the minimum in the $q\bar{q}$ section in Fig. 2 ($q\bar{q}\gamma$) with the minimum in Fig. 5 ($q\bar{q}g$) we see that the

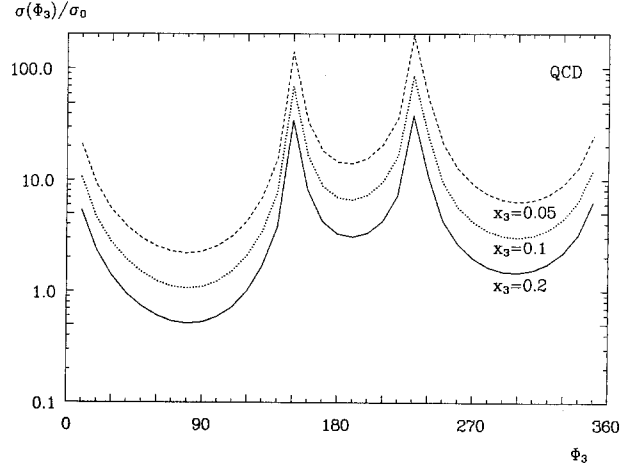


Fig. 5. $\sigma(\phi_3)/\sigma_0$ between q , \bar{q} and g in $q\bar{q}g$ events for $x_3 = 0.05, 0.1$ and 0.2 (complete matrix elements) as a function of ϕ_3

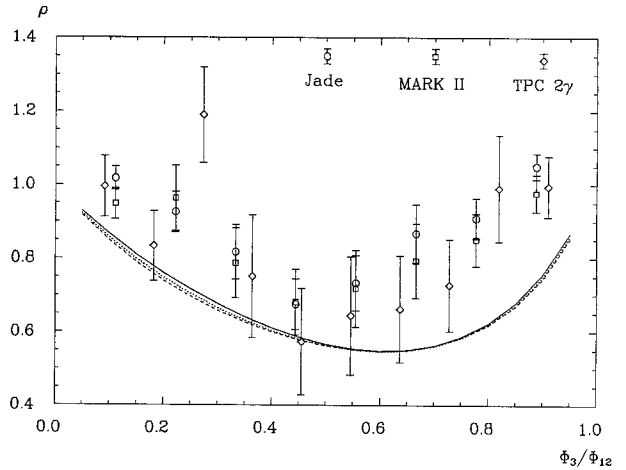


Fig. 6. The ratio ρ of soft parton densities in $q\bar{q}g$ and $q\bar{q}\gamma$ events in the region between q and \bar{q} jets, as a function of the normalized angle ϕ_3/ϕ_{12} compared to data of JADE [11], MARK II [10] and TPC-2 γ [9] collaborations

minimum for the $q\bar{q}g$ case is much deeper than for the $q\bar{q}\gamma$ case [8]. The normalization of the curves is such, that they coincide for very small angles ($\phi_3 \leq 20^\circ$). Of course, the deepening of the minimum for $q\bar{q}g$ originates from the destructive interference in the double pole $1/y_{13}y_{34}$ in (2.14). In Fig. 6 we compare the ratio

$$\rho = \frac{\sigma(\phi_3/\phi_{12})_{q\bar{q}g}}{\sigma(\phi_3/\phi_{12})_{q\bar{q}\gamma}} \quad (2.15)$$

with experimental data coming from the TPC [9], MARK II [10] and JADE [11] collaborations. These data show the corresponding ratio of the particle density in the $q\bar{q}$ region for $q\bar{q}g$ and $q\bar{q}\gamma$ events, where the $q\bar{q}$ region is defined as the region between the two

most energetic jets. This ratio should be 1 if no coherence effects were present, since the gluon and photon energies were chosen in such a way that the kinematical configurations of both event types are similar. Furthermore the relative normalization of the experimental particle distributions agrees with the relative normalization adopted for our theoretical curves. We see the depletion effect is independent of x_3 . The smallest value of ρ is $\rho \simeq 0.5$. This is smaller than the experimental value $\rho \simeq 0.7$. This difference can be easily accounted for. In the experimental data the third jet is the least energetic jet which is not always the gluon jet. The probability that the gluon is the third jet is only 65%. One then expects a depletion of about 35% from our theoretical curves which is in good agreement with the data.

So the model agrees nicely with the data on soft hadron distributions. The relative amount of produced hadrons as a function of ϕ_3 between the jets is predicted qualitatively correctly for the $q\bar{q}\gamma$ and the $q\bar{q}g$ process. A more quantitative comparison is difficult since our results are for soft gluons between the jets whereas the experimental data are for soft hadrons emitted between the jets. The qualitative agreement between our results and the data is consistent with the parton-hadron duality hypothesis.

In the theoretical model the characteristic features originate from the splitting of the gluon jet into two gluons which causes the interference effects with the terms coming from $q \rightarrow qg$ and $\bar{q} \rightarrow \bar{q}g$. But the gluon can also split into $q\bar{q}$. This contribution has only a single pole in y_{34} with a rather small coefficient. Therefore it contributes only a small term to the third peak in Fig. 5. On the other hand in the case of an abelian gluon this would be the only term responsible for the emission of a soft parton from the gluon jet. This case has been calculated in Fig. 7. Here $T_R = 3N_f$, where N_f is the number of flavours, $N_c = 0$ and $C_F = 1$. The extra factor 3 in T_R accounts for the factor 3

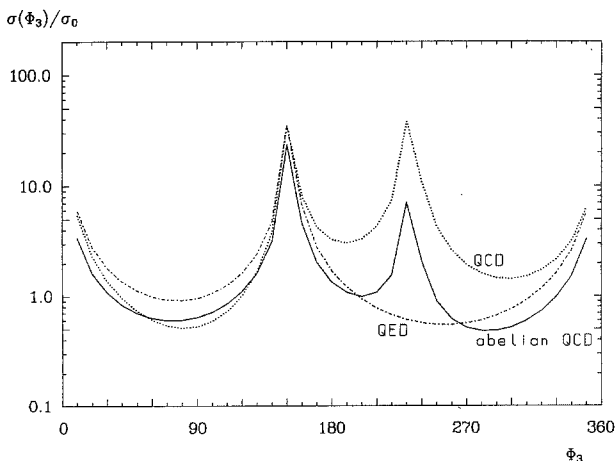


Fig. 7. $\sigma(\phi_3)/\sigma_0$ for $q\bar{q}g$ (QCD), $q\bar{q}\gamma$ (QED) and for $q\bar{q}g$ events in an abelian gluon theory (abelian QCD) as a function of ϕ_3 for $x_3 = 0.2$

missing in σ_0 , if only N_f flavours are considered [19]. Therefore the single pole contribution coming from $g \rightarrow q\bar{q}$ is enhanced by the factor 6 as compared to QCD. This single pole in y_{34} produces a third maximum, as is seen in Fig. 7. But the relative depth of the three minima does not agree with the experimental data. The first and the third minimum are roughly equal and the second minimum lies only slightly higher than the first minimum. From this we conclude that in the QCD model the relative depth of the three minima is directly related to the colour structure of QCD, in particular to the nonabelian nature of QCD.

As we have seen the perturbative QCD matrix elements explain quite nicely the characteristic features of soft hadron emission between jets. In this sense the local parton-hadron duality as introduced in [8] works rather well, which means that the distribution of hadrons follows that of the QCD partons rather closely. Unfortunately this explanation of the “string” effect through parton coherence has an essential drawback. This is the absolute value of the predicted cross sections. In order to compare with the experimental cross section we must integrate our cross section over x_3 . In the experimental distributions only particles with momenta exceeding 150 MeV were used (for example in the JADE experiment [11]). This corresponds to a lower limit in x_3 of roughly 0.01 (if all particles are assumed to be pions). The ϕ_3 -distributions plotted in Fig. 5 behave as a function of x_3 approximately as $1/x_3$ which determines the dependence of the theoretical cross sections on the lower x_3 cut. Then comparing with the JADE cross sections based on $6 \cdot 10^4$ multi-hadronic and 8619 3-jet events, which were used for the experimental distributions [11], we come to the conclusion that our cross sections are too large by a factor of about 20 (this applies also to the $q\bar{q}\gamma$ cross section), if we renormalize the experimental distributions to the total number of hadronic events and divide by the mean particle multiplicity of the selected events. This factor of about 20 equals approximately this mean particle multiplicity. Then to get agreement we argue, that the hadrons between the jets always have the direction of the soft gluon g_3 —this is essentially the assumption of parton-hadron duality—and the non-perturbative fragmentation, which transforms the gluon (or additional soft gluons) into hadrons has no other effect as to produce the correct normalization of the hadronic amplitude in relation to the partonic amplitude. If this is so, one would like to see how this happens in a model which incorporates hadronization of quarks and gluons and the coherence effect in the partonic amplitudes. Of course, there is the possibility that the string comes from the fragmentation, this is the approach of the Lund model [7], and has nothing to do with the properties of the partonic amplitudes (see [9], [10] and [11], where it is shown that the hadron distributions between the jets in $q\bar{q}g$ and $q\bar{q}\gamma$ events are very well accounted for in the Lund model).

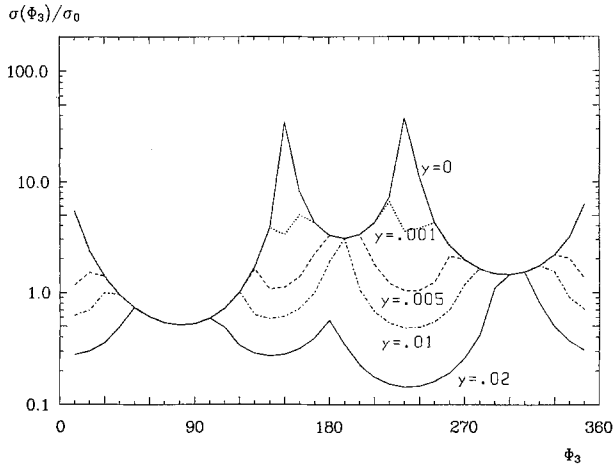


Fig. 8. $\sigma(\phi_3)/\sigma_0$ for $q\bar{q}g$ events calculated from $q\bar{q}gg + q\bar{q}q\bar{q}$ matrix elements supplied with an invariant mass cut y with $y = 0.02, 0.01, 0.005$ and 0.001 as a function of ϕ_3

In order that the coherence does not originate from the hadronization, but truly reflects the partonic nature, we must take one of the independent fragmentation models [3, 4]. In the model 3 (including virtual $O(\alpha_s^2)$ corrections) and 4 partons are generated according to perturbative QCD which then fragment into hadrons according to [3, 4]. Since such a model contains 4-parton production on the basis of amplitudes also used in this work, one might naively expect that the parton coherence effect is also built in. But this is not the case. The reason is that in all these models [15] the 4-parton terms are present only for the production of *hard* partons. The amplitudes for the production, where one of the four partons is *soft*, are combined with the virtual corrections to 3 parton ($q\bar{q}g$) production to cancel infrared and collinear singularities [19]. In this sense the soft parton contributions are already absorbed in the hard jets. How far this absorption takes place depends on the resolution cut which defines the separation of 3 and 4 jets. If we define as usual this separation with invariant mass cuts $(p_i + p_j)^2/q^2 = y_{ij}$ ($i, j = 1, 2, 3, 4$), so that $y_{ij} \geq y$ defines the genuine 4-jet production, we can study how such an invariant mass cut influences the cross section for the production of the soft gluon g_3 . The result is seen in Fig. 8, in which the ϕ_3 distribution for $q\bar{q}g$ production is plotted for four cut values ($y_{i3} \geq y$) $y = 0.001, 0.005, 0.01$ and 0.02 . For fixed x_3 ($x_3 = 0.2$) the constraint $y_{i3} \geq y$ is essentially a constraint on ϕ_3 . Therefore the regions where the ϕ_3 distribution peaks are reduced very much (only non-singular terms remain) and the regions between the jets is also cut out depending on the chosen y value. Experimentally the jet separation is possible if $y \geq 0.02$ [20]. For smaller y values the 4-jet cross section becomes so large that it exceeds the unitarity limit (i.e. 4-jet rate > 1). For $y = 0.02$ the jet peaks in Fig. 8 have disappeared and between the jet peaks (for $y = 0$) the cross section has the original value as for

$y = 0$ in some limited ϕ_3 range. If y is decreased the ϕ_3 ranges between the peaks increase and the peaks gradually are built up again for $y = 10^{-3}$. Even in this case the ϕ_3 distribution differs appreciably from the one with $y = 0$.

In the perturbative model with IF fragmentation and $y \simeq 0.01$ the peaks are restored through the addition of 3-jet production with subsequent hadronization of the 3-jets. This leads to soft hadron distributions for which the first minimum and the third minimum are in the ratio 1:1.5 instead of 1:3 as in Fig. 5, but with the correct normalization if compared to the experimental data (see e.g. [11]). It is conceivable that if y is chosen small enough, i.e. $y \lesssim 5 \cdot 10^{-3}$, the pattern of minima, obtained for soft gluon emission, is still present after hadronization and the correct normalization is obtained and thus would explain the coherence effect observed experimentally. In order this to happen the artificial maxima near $\phi_3 = 90^\circ, 180^\circ$ and 300° in Fig. 8 must be levelled to the correct normalization without changing the relative normalization in the three ϕ_3 regions through fragmentation of the soft gluon. How this might happen will be studied in future work.

3 Summary and concluding remarks

We have calculated the cross section for soft gluon emission in $e^+e^- \rightarrow q\bar{q}\gamma g$ and $e^+e^- \rightarrow q\bar{q}gg$ by evaluating the complete 4-parton matrix elements. We find the coherence pattern as predicted by Azimov et al. [8] for the angular distribution of the soft gluon. Our results differ from the approximate eikonal formulas (for gluon momentum going to zero) by less than 30%. It is pointed out that the coherence of soft gluon radiation agrees with the observed distribution for hadron emission between the hard jets in $e^+e^- \rightarrow q\bar{q}\gamma$ and $e^+e^- \rightarrow q\bar{q}g$. The observed interference pattern is characteristic for the non-abelian nature of QCD and does not come out in an abelian gluon theory.

Due to the infrared singular behaviour the cross section for soft gluon emission is a factor of 20 too large. Therefore the parton-hadron duality [8] is only qualitatively in agreement with experimental results and it is to be shown how the hadronization of the soft gluon and the hard jets can change the normalization. The infrared singular behaviour is also responsible for the fact that the coherence effects contained in the 4-parton production cross section are not present in the models for high energy hadron production based on $O(\alpha_s^2)$ perturbation theory and subsequent independent fragmentation. In these models the infrared part of $e^+e^- \rightarrow q\bar{q}gg$ is part of the production of three hard, although dressed, jets. Then the information contained in $e^+e^- \rightarrow q\bar{q}gg$ is lost and no predictions about details of soft gluon emission inside jets are possible. It would be desirable to rescue the coherence of soft gluon emission in

$e^+e^- \rightarrow q\bar{q}gg$ for the model building for hadron production in e^+e^- annihilation.

Acknowledgements. We thank W. Hofmann for correspondence and R. Felst and F. Ould Saada for discussions concerning the experimental results. Fruitful discussions with V. A. Khoze are gratefully acknowledged.

References

1. Recent reviews are: Sau Lan Wu: Phys. Rep. 107 (1984) 59; F. Barreiro: Fortschr. Phys. 34 (1986) 503; J. Dorfan: Proceedings of 1986 SLAC Summer Institute, Stanford, Calif. 1986, SLAC-PUB-4287, (1987); W. de Boer, SLAC-PUB-4428 (1987)
2. R.D. Field, R.P. Feynman: Nucl. Phys. B136 (1978) 1
3. P. Hoyer et al.: Nucl. Phys. B161 (1979) 1
4. A. Ali et al.: Phys. Lett. B93 (1980) 155
5. W. Bartel et al.: Z. Phys. C—Particles and Fields 21 (1983) 37; Phys. Lett. B134 (1984) 275; Phys. Lett. B157 (1985) 340
6. H. Aihara et al.: Z. Phys. C—Particles and Fields 28 (1985) 31; M. Althoff et al.: Z. Phys. C—Particles and Fields 29 (1985) 29
7. B. Anderson et al.: Phys. Rep. 97 (1983) 31 and earlier references given there
8. Y.I. Azimov et al.: Phys. Lett. B165 (1985) 147
9. H. Aihara et al.: Phys. Rev. Lett. 57 (1986) 945
10. P.D. Sheldon et al.: Phys. Rev. Lett. 57 (1986) 1398
11. F. Ould Saada et al.: DESY report 88-015 (1988) and Z. Phys. C—Particles and Fields 39 (1988) 1
12. G. Marchesini, B.R. Webber: Nucl. Phys. B238 (1984) 1; B.R. Webber: Nucl. Phys. B238 (1984) 492
13. T.D. Gottschalk: Nucl. Phys. B214 (1983) 201
14. R.K. Ellis, G. Marchesini, B.R. Webber: Nucl. Phys. B286 (1987) 643 and the earlier literature given there
15. See for example: T. Sjöstrand: Comput. Phys. Commun. 27 (1982) 243; 28 (1983) 229; Z. Phys. C—Particles and Fields 26 (1984) 93
16. K. Fabricius et al.: Z. Phys. C—Particles and Fields 11 (1982) 315
17. A. Ali et al.: Nucl. Phys. B167 (1980) 454; J.G. Körner et al.: Nucl. Phys. B185 (1981) 365; R.K. Ellis et al.: Nucl. Phys. B178 (1981) 421
18. G. Kramer, B. Lampe: DESY report 86-119 (1986) (unpublished) to be published in Fortschr. Phys.
19. G. Kramer: Springer Tracts in Modern Physics, Vol. 162. Berlin, Heidelberg, New York: Springer 1984
20. W. Bartel et al.: Z. Phys. C—Particles and Fields 33 (1986) 23